ACS Catalysis

LETTER

pubs.acs.org/acscatalysis

Differences in Catalytic Sites for CO Oxidation and Propylene Epoxidation on Au Nanoparticles

Wen-Sheng Lee,[†] Rong Zhang,[†] M. Cem Akatay,[‡] Chelsey D. Baertsch,[†] Eric A. Stach,[‡,§] Fabio H. Ribeiro,[†] and W. Nicholas Delgass*[,†]

[†]Forney Hall of Chemical Engineering, Purdue University, 480 Stadium Mall Drive, West Lafayette, Indiana 47907, United States

[‡]School of Materials Engineering and Birck Nanotechnology Center, Purdue University, West Lafayette, Indiana 47907, United States

[§]Center for Functional Nanomaterials, Brookhaven National Laboratory, Upton, New York 11973, United States

Supporting Information

ABSTRACT: Sintering and increased Au loading of Au/TS-1 causes the rate of CO oxidation per mole of Au to increase, whereas that for epoxidation of propylene in O_2 and H_2 decreases. This opposite trend in rate behavior shows that the catalytic sites for the two reactions must be different.

KEYWORDS: propylene epoxidation, CO oxidation, Au/TS-1, gold active site

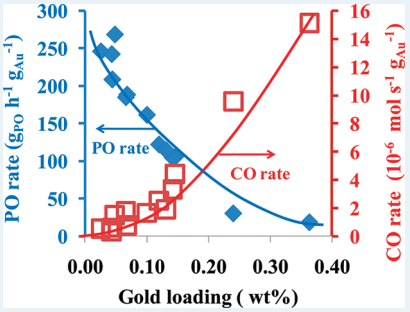

The unexpectedly high reaction rate of gold catalysts in many systems, such as CO oxidation, water gas shift (WGS) reaction, and gas phase epoxidation of propylene by O_2 plus H_2 (PO reaction),[1−6] has focused research toward an understanding of the nature of the active sites that can support the design of the next generation of catalysts. The gold particle size and the type of support have been shown to be two of the key factors that control the performance of gold catalysts.[1,2,7] The fact that CO oxidation and WGS reaction rates scale with approximately $1/d^3$ (d represents the gold particle diameter) for Au/TiO_2 suggests that small gold particles (<5 nm) are indispensible for the high activity.[5,8,9] However, this rate dependence on gold particle size can also be strongly affected by the type of support. The variation in CO oxidation rate for silica-supported gold catalysts with gold particle sizes spanning from ∼2 to ∼30 nm is much smaller compared with that of titania-supported gold catalysts with a similar gold particle size range.[9] Therefore, both the effect of the support and the gold particle size have to be taken into account in studies of the active sites on gold catalysts.

Early studies suggested that the optimum gold particle size for CO oxidation ranges from 2−5 nm.[1,2,10] Interestingly, for the TiO_2 support, a similar optimum gold particle size range was proposed for the PO reaction as well.[2] On the other hand, titanium silicate-1 (TS-1) has been selected as an alternative support for PO catalysts because its higher Ti dispersion and tetrahedral coordination result in higher rates and better stability.[3,4,11] Our previous experimental data, together with density functional theory (DFT) calculation results, suggest that gold clusters smaller than 2 nm in Au/TS-1 can be responsible for the high PO activity.[4,6,12−14] Recently, Huang et al.[15,16] also suggested that gold clusters smaller than 2 nm on the external surface of TS-1 are the dominant active gold sites for the PO reaction. Although it is often presumed that the catalytic site for CO oxidation is the same as that for the PO reaction, this issue has not been addressed for the Au/TS-1 system. The work presented here provides direct evidence that demonstrates that the gold catalytic sites for CO oxidation and the PO reaction are different for Au/TS-1. For the TS-1 support, the optimum gold particle size for CO oxidation is confirmed to be in the region of 2−5 nm, whereas gold clusters smaller than 2 nm are the dominant active species for the PO reaction.

TS-1, with Si/Ti (molar ratio) = 100, was prepared according to the method of Khomane et al.[17] Au/TS-1 was prepared by using the deposition−precipitation (DP) method.[4] Detailed information about the material preparation and characterization as well as the kinetic measurements is provided in the Supporting Information (SI). The pH of the gold slurry solution was kept at ∼7 during DP to minimize the effects of residual chlorine, sodium, or both on the catalytic performance in both reactions. At pH ∼ 7, most of the chlorine coordinated to the gold complex was replaced by hydroxyl groups.[18] The catalysts were named as 0.048Au/TS-1(100), where 0.048 represents the gold loading in weight percent and 100 represents the Si/Ti molar ratio in TS-1. Both PO and CO catalytic activities were determined using a plug flow reactor at differential conversion. The external mass transfer effects on the rates were minimized by operating at high space velocity (14 000 mL h^{-1} g_{cat}^{-1}). Internal mass transfer

Received: July 13, 2011
Revised: August 29, 2011
Published: August 29, 2011

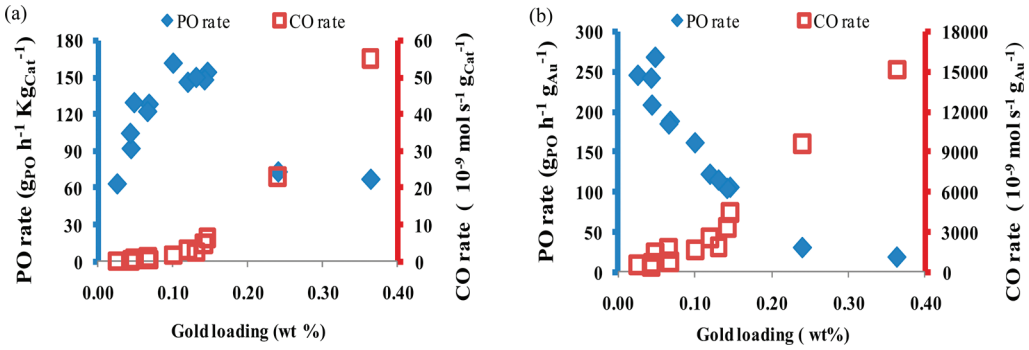

Figure 1. PO/CO rate, normalized by (a) the amount of catalyst, (b) the amount of gold, as a function of gold loading (wt %). The data (for both PO/CO) were taken as the average values between the third and fifth hours at 200 °C, 0.05/0.025/bal (vol %) = CO/O_2/He or 10/10/10/70 vol % = $C_3H_6/H_2/O_2/N_2$, and space velocity = 14 000 mL h^{-1} g_{cat}^{-1}.

limitations can be neglected because the estimated Thiele modulus is smaller than 1 (see SI). Typical PO/CO rate-vs-time-on-stream data are also available (Figures S10, S11 of the SI).

Figure 1a presents both the PO and CO rates on Au/TS-1 catalysts with different gold loadings. For the PO reaction, there are two regions in Figure 1a. When the gold loading is lower than ~0.05 wt %, the PO rate (g_{PO} h^{-1} kg_{cat}^{-1}) is approximately linear in gold loading, suggesting that the number of active sites for PO also increases linearly as the gold loading increases in this region. When the gold loading is higher than 0.07 wt %, the PO rate (g_{PO} h^{-1} kg_{cat}^{-1}) reaches a plateau, indicating that the extra gold does not provide any additional active sites. Further increase in the gold loading from ~0.15 to ~0.36 wt %, achieved by increasing the catalyst preparation temperature, lowers the PO catalytic performance. Renormalization of the PO rate by the amount of gold shows that the gold atom efficiency (g_{PO} h^{-1} g_{Au}^{-1}) decreases as the gold loading increases above 0.05 wt %, as shown in Figure 1b. On the basis of the assumption that the gold particle size generally increases with gold loading,[6] the significant decrease in the gold atom efficiency suggests the catalytic site for PO is size-sensitive and that the most active gold clusters are very small.

As to PO selectivity, it generally decreases as the gold loading increases. However, the difference is small (Figure S1a, SI), and the error in the PO selectivity measurement is discussed in the SI. Therefore, the correlation of the propylene rate with gold loading is similar to the one between the PO rate and the gold loading (Figure S1b, SI). For CO oxidation, Figure 1a, two separate regions of behavior can also be identified. When the gold loading is lower than ~0.12 wt %, the CO oxidation rate (mol s^{-1} g_{cat}^{-1}) shows a slow increase with gold loading. However, instead of reaching a plateau, as for the PO reaction, further increase of the gold loading (0.12 to 0.36 wt %) drastically increases the CO oxidation rate. The gold atom efficiency (mol s^{-1} g_{Au}^{-1}) also increases as the gold loading increases. This implies that the larger gold particles (>1 nm) might be more active than the small ones for CO oxidation. This hypothesis has been tested by the experiments discussed below.

Previous experimental results show that the gold loading roughly tracks the Ti content in the TS-1.[4] DFT calculations also suggest that a defect site/Ti pair in the TS-1 might be a possible anchor site for deposition of gold clusters.[14,19] If the assumption is made that one Ti atom can accommodate one gold atom, the corresponding gold loading would be ~3.3%. Even if only the external surface area of the TS-1 is considered, and we assume that ~1% of the bulk Ti content is on the external surface (corresponding to the measured TS-1 crystallite size of 281 nm; see Figure S3 of the SI), it would take about 3 gold atoms per Ti to reach a gold loading of 0.1 wt %. Therefore, there are ample Ti sites to accommodate the gold particles. In addition, TEM analysis of the fresh Au/TS-1 sample with 0.066 wt % gold loading shows no visible gold particles on the TS-1 (Figure S6, SI). This simple calculation, together with the TEM analysis, suggests that gold clusters much smaller than 2 nm are highly dispersed over the TS-1 in the freshly made samples. However, no further information about the location or structural features of the active gold clusters in the Au/TS-1 is available on the basis of the data presented here.

During the reaction at 200 °C, aggregation of the small gold clusters could be significant because of the known decrease in melting point of gold at decreasing gold particle size.[20] At low gold loading, the small gold clusters, which are active for the PO reaction but relatively inactive for CO oxidation, can still maintain their small size because of their high dispersion. The distance between gold clusters may be sufficient to diminish the gold cluster sintering effect. As the gold loading increases, both the population of small gold clusters and the size of the clusters would increase. At reaction temperature, the gold clusters might tend to migrate and to form larger gold particles. When the gold particle size is larger than 1 nm, it is too large to fit inside the TS-1 channels. Therefore, these larger gold particles are expected to be on the external surface of TS-1

On the basis of the fact that very low CO oxidation rates were observed for the samples with low gold loadings, we assume that the CO oxidation activity comes mainly from the existence of larger gold particles formed by the aggregation/migration from small gold clusters originally dispersed on the TS-1. Several samples with different gold loadings were chosen for TEM analysis (see Figures S4–S8 of the SI). We selected two samples with different gold loadings but with similar average gold particle sizes and particle size distribution to test this hypothesis because the CO oxidation rate (mol s^{-1} g_{cat}^{-1}) would scale with the population of the visible (large) gold particles (>1 nm) regardless of what the actual active sites (perimeter, corner, etc) are. Figure S9 of the SI shows a good correlation between the CO oxidation rate (mol s^{-1} g_{cat}^{-1}) and the density of visible gold particles (>1 nm) for the two selected samples (0.048Au/TS-1(100) and 0.12Au/TS-1(100)), indicating the CO oxidation rate is dominated by the visible large gold particles with average size around 2.8 nm.

dx.doi.org/10.1021/cs200373f |ACS Catal. 2011, 1, 1327–1330

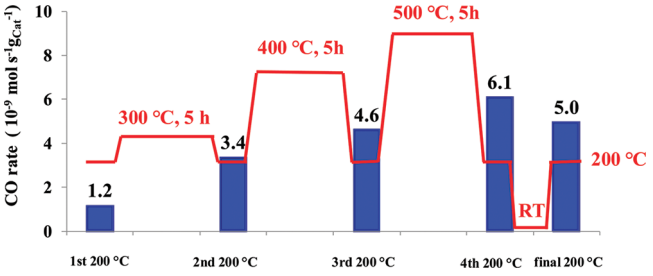

Figure 2. Sintering protocol and corresponding CO oxidation rate at 200 °C for 0.066Au/TS-1(100).

To reinforce the argument that the catalytic sites for the PO reaction and CO oxidation are different, individual sintering experiments were carried out for each reaction. For CO oxidation, the catalyst (0.066Au/TS-1(100)) was intentionally sintered at three different temperatures—300, 400, and 500 °C—under CO oxidation reaction conditions. Each sintering step lasted for 5 h, and then the reaction temperature was lowered to 200 °C to test the effect of gold particle sintering on the rate. After the full sintering sequence, the catalyst was cooled to room temperature in the reaction mixture overnight, and the activity was retested at the reaction temperature of 200 °C (final bar in Figure 2). For the PO reaction, the catalyst (0.04Au/TS-1(127)) was subjected to only one sintering temperature, 318 °C, for 6 h under PO reaction conditions. To avoid the effect of residual carbon that was generated during the reaction/sintering step, the reaction mixture was switched to an oxygen/nitrogen mixture to burn off the possible residual carbon before and after the sintering step at 318 °C. Figure 2 shows the sintering temperature protocol as well as the effect of the gold particle sintering on the CO oxidation rate. The CO oxidation rate at 200 °C after each sintering step, from 300 to 500 °C, always increased. The monotonic increase in the CO oxidation after each sintering step strongly suggests that the gold particles with large size are the active sites for CO oxidation. The decrease in the CO oxidation rate at the final stage can be attributed to further sintering of the gold particles, which resulted in gold particles large enough to diminish the total number of active sites per gram of catalyst. The TEM images show that the mean gold particle size of this sample (0.066Au/TS-1(100)) after the sintering experiments was ~4.7 nm.

This particle size effect was confirmed by plotting the relationship between CO oxidation rate (mol s^{-1} g_{Au}^{-1}) and the gold particle size. Three selected samples—0.048Au/TS-1(100), 0.12Au/TS-1(100), and 0.36Au/TS-1(100)—together with the sample from the sintering experiment, were chosen for this plot. Figure S13 of the SI, shows that the gold atom efficiency for CO oxidation reaches a maximum at ~3.5 nm. This optimum range is in good agreement with the data at lower temperatures for Au on nonmesoporous SiO_2 catalysts published in the literature.[21] For the PO reaction, it was found that after sintering, the activity drastically dropped by ~55% compared with the activity before sintering, as shown in Figure S12a of the SI. This large drop in activity after the sintering step supports the idea that large gold particles are not the active sites for the PO reaction, whereas the PO selectivity was found to be insensitive to the particle size, as evidenced by the small change before and after the sintering step (Figure S12b of the SI).

Exact comparison of our measured rates for CO oxidation to literature values is difficult because there are no reported values for Au on nanoporous silica or values obtained at our reaction conditions on any silica-based supports. Furthermore, variations in reported reaction orders and activation energies for silica-based catalysts also make extrapolation difficult.[22] Nevertheless, our rates are within an order of magnitude of these reported for a Au/mesoporous silica catalyst.[23] Our PO rates in the range of 150 g_{PO} h^{-1} kg_{cat}^{-1} are also in accord with those recently reported.[15,16]

CONCLUSIONS

This work shows that the catalytic sites for CO oxidation and PO reactions are different. The active gold particles for CO oxidation range from 2 to 5 nm, whereas much smaller gold clusters, <2 nm, are the dominant active sites for PO reaction in Au/TS-1 system. Correspondingly, as the particles grow large, the CO rate increases but that for PO decreases.

ASSOCIATED CONTENT

Supporting Information. This material is available free of charge via the Internet at http://pubs.acs.org.

AUTHOR INFORMATION

Corresponding Author

*Phone: 765 494 4059. Fax: 765 494 0805. E-mail: delgass@purdue.edu.

ACKNOWLEDGMENT

Support from the Department of Energy, Office of Basic Energy Sciences, Chemical Sciences, under Grant DE-FG02-03ER15408 is gratefully acknowledged.

REFERENCES

(1) Haruta, A. *Chem. Rec.* **2003**, *3*, 75–87.
(2) Haruta, M.; Date, M. *Appl. Catal., A* **2001**, *222*, 427–437.
(3) Stangland, E. E.; Stavens, K. B.; Andres, R. P.; Delgass, W. N. *J. Catal.* **2000**, *191*, 332–347.
(4) Taylor, B.; Lauterbach, J.; Delgass, W. N. *Appl. Catal., A* **2005**, *291*, 188–198.
(5) Williams, W. D.; Shekhar, M.; Lee, W. S.; Kispersky, V.; Delgass, W. N.; Ribeiro, F. H.; Kim, S. M.; Stach, E. A.; Miller, J. T.; Allard, L. F. *J. Am. Chem. Soc.* **2010**, *132*, 14018–14020.
(6) Yap, N.; Andres, R. P.; Delgass, W. N. *J. Catal.* **2004**, *226*, 156–170.
(7) Kung, M. C.; Davis, R. J.; Kung, H. H. *J. Phys. Chem. C* **2007**, *111*, 11767–11775.
(8) Janssens, T. V. W.; Clausen, B. S.; Hvolbaek, B.; Falsig, H.; Christensen, C. H.; Bligaard, T.; Norskov, J. K. *Top. Catal.* **2007**, *44*, 15–26.
(9) Lopez, N.; Janssens, T. V. W.; Clausen, B. S.; Xu, Y.; Mavrikakis, M.; Bligaard, T.; Norskov, J. K. *J. Catal.* **2004**, *223*, 232–235.
(10) Valden, M.; Lai, X.; Goodman, D. W. *Science* **1998**, *281*, 1647–1650.
(11) Mul, G.; Zwijnenburg, A.; van der Linden, B.; Makkee, M.; Moulijn, J. A. *J. Catal.* **2001**, *201*, 128–137.
(12) Joshi, A. M.; Delgass, W. N.; Thomson, K. T. *J. Phys. Chem. B* **2005**, *109*, 22392–22406.
(13) Joshi, A. M.; Delgass, W. N.; Thomson, K. T. *J. Phys. Chem. B* **2006**, *110*, 23373–23387.
(14) Joshi, A. M.; Delgass, W. N.; Thomson, K. T. *J. Phys. Chem. C* **2007**, *111*, 7841–7844.

(15) Huang, J. H.; Lima, E.; Akita, T.; Guzman, A.; Qi, C. X.; Takei, T.; Haruta, M. *J. Catal.* **2011**, *278*, 8–15.
(16) Huang, J. H.; Takei, T.; Akita, T.; Ohashi, H.; Haruta, M. *Appl. Catal., B* **2010**, *95*, 430–438.
(17) Khomane, R. B.; Kulkarni, B. D.; Paraskar, A.; Sainkar, S. R. *Mater. Chem. Phys.* **2002**, *76*, 99–103.
(18) Moreau, F.; Bond, G. C.; Taylor, A. O. *J. Catal.* **2005**, *231*, 105–114.
(19) Wells, D. H.; Delgass, W. N.; Thomson, K. T. *J. Am. Chem. Soc.* **2004**, *126*, 2956–2962.
(20) Buffat, P.; Borel, J. P. *Phys. Rev. A* **1976**, *13*, 2287–2298.
(21) Veith, G. M.; Lupini, A. R.; Rashkeev, S.; Pennycook, S. J.; Mullins, D. R.; Schwartz, V.; Bridges, C. A.; Dudney, N. J. *J. Catal.* **2009**, *262*, 92–101.
(22) Aguilar-Guerrero, V.; Gates, B. C. *Catal. Lett.* **2009**, *130*, 108–120.
(23) Chi, Y. S.; Lin, H. P.; Mou, C. Y. *Appl. Catal., A* **2005**, *284*, 199–206.